Thermoresponsive Triblock Copolymer Aggregates Investigated by Laser Light Scattering

ARTICLE *in* THE JOURNAL OF PHYSICAL CHEMISTRY B · JUNE 2007

Impact Factor: 3.3 · DOI: 10.1021/jp0659352 · Source: PubMed

3 AUTHORS:

Xuechang Zhou
Shenzhen University
29 PUBLICATIONS **445** CITATIONS
SEE PROFILE

Xiaodong Ye
University of Science and Technology of China
50 PUBLICATIONS **880** CITATIONS
SEE PROFILE

Guangzhao Zhang
University of Science and Technology of China
203 PUBLICATIONS **4,082** CITATIONS
SEE PROFILE

Thermoresponsive Triblock Copolymer Aggregates Investigated by Laser Light Scattering

Xuechang Zhou, Xiaodong Ye, and Guangzhao Zhang*

Hefei National Laboratory for Physical Sciences at Microscale, Department of Chemical Physics, University of Science and Technology of China, Hefei, Anhui, China

Received: September 12, 2006; In Final Form: February 12, 2007

Narrowly distributed polystyrene−*b*-poly(*N*-isopropylacrylamide)−*b*-polystyrene (PS−*b*-PNIPAM−*b*-PS) triblock copolymer with trithiocarbonate group in the middle of PNIPAM block was synthesized by using reversible addition fragmentation chain transfer (RAFT) polymerization. Such copolymer chains form a micelle-like aggregate with PNIPAM interlocking rings and associating PS blocks as the core and PNIPAM rings as the corona. The hydrolysis of the trithiocarbonate group leads the rings in the corona to be cut into open linear coils. Using laser light scattering, we have investigated the temperature-induced collapse of the aggregates with the rings and coils in the corona. Our results reveal that the former shrink much less than the latter due to the topological effect of PNIPAM blocks in the corona. On the other hand, the aggregates with long coils exhibit a sharper collapse transition than those with shorter coils.

Introduction

Polymer chains grafted on surface exhibit rich conformations, depending on the grafting density, the solvent quality, and the polymer−surface interaction.[1−5] For example, the chains form polymer brush when the grafting density is high enough. It has been predicted that polymer brushes exhibit a continuous collapse due to the constraint of the chains.[6,7] Experimentally, some investigations demonstrate that such a collapse is indeed gradual,[8−11] but the others show the transition is sharp.[12,13] In our previous study,[14] using micelles and vesicles made of polystyrene−*b*-poly(*N*-isopropylacrylamide) (PS−*b*-PNIPAM) diblock copolymers, we investigated the temperature-induced conformational change of PNIPAM chains tethered on convex and concave surfaces. Our results reveal that PNIPAM chains on a convex surface exhibit a broaden collapse transition, whereas PNIPAM chains on a concave surface have a discontinuous transition. The conformation of grafted polymer chains has great effect on the surface properties. It is also significant for the dynamics of biomolecules captured on the membrane of a cell.[15]

In the present study, we have prepared narrowly distributed polystyrene−*b*-poly(*N*-isopropylacrylamide)−*b*-polystyrene (PS−*b*-PNIPAM−*b*-PS) triblock copolymer with trithiocarbonate group in the middle of PNIPAM block using reversible addition fragmentation chain transfer (RAFT) polymerization.[16−18] The triblock copolymer chains form micelle-like aggregates in water at 20 °C with PNIPAM rings as the corona. The trithiocarbonate group can be hydrolyzed into thiol group by $NaBH_4$ in aqueous solution at room temperature,[19] so that a PNIPAM ring is cut into two linear coils (Scheme 1). Here, we report the temperature-induced collapse of the aggregates with either rings or coils grafted on the same surface by use of laser light scattering (LLS).

SCHEME 1: Transformation of a Flower-Like Aggregate to a Star-Like Aggregate

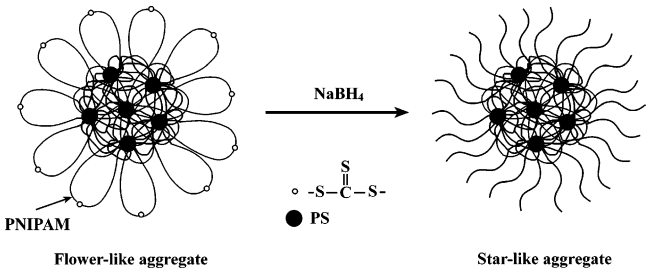

Experimental Section

Materials. Styrene was distilled under reduced pressure after it was washed with an aqueous solution of sodium hydroxide (5 wt %) three times and then with water until neutralization. It was dried over anhydrous calcium chloride and then distilled under reduced pressure before use. *N*-isopropylacrylamide (NIPAM) from Aldrich was purified by recrystallization from a mixture of benzene and *n*-hexane. 4,4′-azobis(isobutyronitrile) (AIBN) from Fluka was purified by recrystallization from ethanol. Tetrahydrofuran (THF) was distilled from a purple sodium ketyl solution. Ethyl-2-bromobutyrate was prepared from the esterification reaction of ethanol and 2-bromobutyric acid. Anionic exchange resin 717 (Shanghai Chemical Reagent Co.) was continuously washed with an aqueous solution of sodium hydroxide (5 wt %) for 24 h and deionized water until neutralization, and then dried in a vacuum oven at 60 °C. Other reagents were used as received.

^{1}H NMR spectra were measured on a Bruker DMX-300 NMR spectrometer using chloroform-*d* ($CDCl_3$) as the solvent and tetramethylsilane (TMS) as the internal standard. Gel permeation chromatographer (GPC) on a Waters 1515 was used to determine the molecular weight and the molecular weight distribution (M_w/M_n) of a polymer with a series of monodisperse polystyrenes as the calibration standard and THF as the eluent with a flow rate of 1.0 mL/min.

Synthesis of PS−*b*-PNIPAM−*b*-PS Triblock Copolymer. A PS−*b*-PNIPAM−*b*-PS triblock copolymer with trithiocarbonate group in the middle of the chain was prepared via RAFT polymerization using s,s′-bis(2-ethyl-2′-butyrate) trithiocarbonate (BEBT) as the chain transfer agent.[16−18] BEBT was prepared

* To whom correspondence should be addressed.

10.1021/jp0659352 CCC: $37.00
Published on Web 04/14/2007

following a procedure in reference 18. After 25 g of dried anionic exchange resin was added into 100 mL of carbon disulfide, the mixture was stirred at room temperature for about 30 min so that the resin turned from yellow to blood red indicating the formation of CS_3^{2-} on the polymeric support. Then, 4.4 g of ethyl-*2*-bromobutyrate was introduced. The mixture was refluxed for 12 h until the solution turned yellow. After the completion of the reaction, the resin was filtered out and carbon disulfide was removed by evaporation under reduced pressure to yield 1 g of a viscous yellow liquid (BEBT). ^{1}HNMR (300 MHz, $CDCl_3$), δ(TMS, ppm): 1.06 (CH_3CH_2CH-), 1.29 (CH_3CH_2O-), 2.03 (CH_3CH_2CH-), 4.25 (CH_3CH_2O-), 4.72 (CH_3CH_2CH-).

Into a 10 mL glass tube were added styrene, AIBN, and BEBT. After three freeze-vacuum-thaw cycles, the tube was sealed under vacuum and then placed in a thermostated bath at 70 °C for 5 h. The resultant PS was precipitated into ethanol, filtered, and then dried in a vacuum oven at 40 °C for 24 h. ^{1}HNMR (300 MHz, $CDCl_3$), δ(TMS, ppm): 7.31−6.30 (aromatic protons), 2.21−1.29 (CH_2CH). M_n (GPC) = 3096, M_w/M_n (GPC) = 1.06.

PS−*b*-PNIPAM−*b*-PS triblock copolymer was synthesized by RAFT polymerization with PS precursor, NIPAM, AIBN, and THF in a 10 mL glass tube. After three freeze-vacuum-thaw cycles, the tube was sealed under vacuum and then placed in a thermostated bath at 70 °C for 6 h. The polymer was precipitated into petroleum ether (bp 30−60 °C). Precipitation was repeated three times, and the polymer was dried at 40 °C in a vacuum oven for 24 h. ^{1}HNMR (300 MHz, $CDCl_3$), δ(TMS, ppm): 7.31−6.30 (aromatic protons), 4.01 [NHCH $(CH_3)_2$], 2.42−1.29 (CH_2CHCO, CH_2CH), 1.20 (NHCH $(CH_3)_2$). Molecular weight of the PNIPAM block was calculated from the intensities of the characteristic peaks in ^{1}HNMR together with the molecular weight of PS block measured by GPC. The triblock copolymers are designated as PS_i−*b*-$PNIPAM_j$−*b*-PS_i, where *i* and *j* are the numbers of styrene and NIPAM units, respectively. For PS_{30}−*b*-$PNIPAM_{39}$−*b*-PS_{30}, M_w/M_n = 1.12. For PS_{30}−*b*-$PNIPAM_{157}$−*b*-PS_{30} with a longer PNIPAM block, M_w/M_n = 1.19.

Preparation of Polymeric Aggregates. The self-assembly of PS−*b*-PNIPAM−*b*-PS was induced by adding a 5 mL solution of PS−*b*-PNIPAM−*b*-PS (1 mg/mL) in THF dropwise into 40 mL of Milli-Q water under stirring at 10 °C. As the mixing progressed, the insoluble PS blocks gradually contracted and associated, while soluble PNIPAM blocks tended to stay on the periphery, leading to the flower-like aggregates with PNIPAM rings as the corona. The resulting solution was dialyzed against Milli-Q water using a semipermeable membrane with cutoff molar masses of 3500 g/mol for 3 days to remove the THF.

After 40 μL of aqueous solution of $NaBH_4$ with a concentration of 0.1 mol/L was added into 20 mL of the above aggregate dispersion with a concentration of 9.3×10^{-5} g/mL, the mixture was stirred at room temperature for 1 week so that the trithiocarbonate groups were hydrolyzed, yielding to the star-like aggregates with PNIPAM coils as the corona.

Laser Light Scattering. LLS measurements were conducted on an ALV/DLS/SLS-5022F spectrometer equipped with a multi-τ digital time correlation (ALV5000) and a cylindrical 22 mW UNIPHASE He−Ne laser (λ_0 = 632 nm) as the light source. In static LLS,[20,21] the weight-average molar mass (M_w), the root-mean-square radius of gyration $\langle R_g^2\rangle_z^{1/2}$ (or written as $\langle R_g\rangle$), and the second virial coefficient A_2 were obtained from the angular dependence of the absolute excess time-average

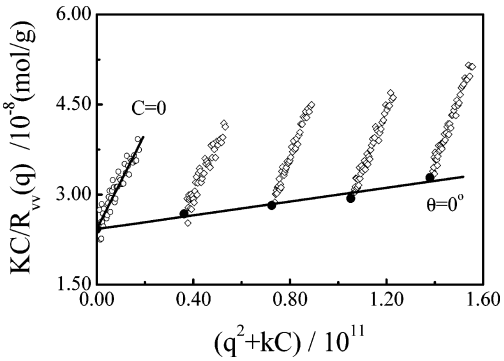

Figure 1. Typical Zimm plot of PS_{30}−*b*-$PNIPAM_{157}$−*b*-PS_{30} flower aggregates in water at 20 °C, where the concentration ranges from 4.7×10^{-6} to 1.80×10^{-5}g/mL.

scattering intensity, known as the Rayleigh ratio $R_{vv}(q)$ by using

$$\frac{KC}{R_{vv}(q)} \approx \frac{1}{M_w}\left(1 + \frac{1}{3}\langle R_g^2\rangle_z q^2\right) + 2A_2C \qquad (1)$$

where $K = 4\pi^2 n^2 (dn/dC)^2/(N_A\lambda_0^4)$ and $q = (4\pi n/\lambda_0)\sin(\theta/2)$, with C, dn/dC, N_A, and λ_0 being concentration of the polymer, the specific refractive index increment, the Avogadro's number, and the wavelength of light in vacuum, respectively. In dynamic LLS,[22] we were able to measure the intensity−intensity time correlation function $G^{(2)}(t,q)$. $G^{(2)}(t,q)$ can be related to the normalized first-order electric field-electric field time correlation function ($|g^{(1)}(t,q)| \equiv \langle E(0,q)\, E(t,q)\rangle$) as

$$G^{(2)}(t,q) = \langle I(0,q)I(t,q)\rangle = A[1 + \beta|g^{(1)}(t,q)|^2] \qquad (2)$$

where t is the delay time, A is the measured baseline; β is an instrument constant depending on the optical coherence of the detection. Generally, $|g^{(1)}(t,q)|$ is related to a characteristic line-width distribution $G(\Gamma)$ as

$$|g^{(1)}(t,q)| = \int G(\Gamma)e^{-\Gamma t}\, d\Gamma \qquad (3)$$

For diffusive relaxation, Γ is related to the translational diffusion coefficient (D) of the scattering object (polymer chain or colloid particle) in dilute solution or dispersion by

$$\Gamma/q^2 = D(1 + Cq^2 < R_g^2 > + \cdots) \qquad (4)$$

where the coefficient (C) depends upon the structure and hydrodynamic interactions of the scattering object. Equation 4 yields $(\Gamma/q_2)_{q\to 0, C\to 0} = D$. Hydrodynamic radius ($R_h$) is obtained by the Stokes−Einstein equation, $R_h = k_BT/6\pi\eta D$, where η, k_B and T are the solvent viscosity, the Boltzmann constant, and the absolute temperature, respectively. For a narrowly distributed system, the cumulant analysis of $|g^{(1)}(t,q)|$ is sufficient to generate in a reliable average $\langle\Gamma\rangle$ or $\langle D\rangle$ or $\langle R_h\rangle$. Hydrodynamic radius distribution $f(R_h)$ was calculated from the Laplace inversion of a corresponding measured $G^{(2)}(t,q)$ using the CONTIN program in the correlator on the basis of eqs 1−3. All dynamic LLS experiments were carried out at a scattering angle of 15°. All the dispersions were clarified using a 0.45 μm Millipore filter. The refractive index increments of the polymeric aggregates were calculated using an addition method.[23]

Results and Discussion

Figure 1 shows a typical Zimm plot for PS_{30}−*b*-$PNIPAM_{157}$−*b*-PS_{30} aggregates at 20 °C before the hydrolysis. On the basis of eq 1, the weight-average molar mass ($M_{w,a}$), average radius

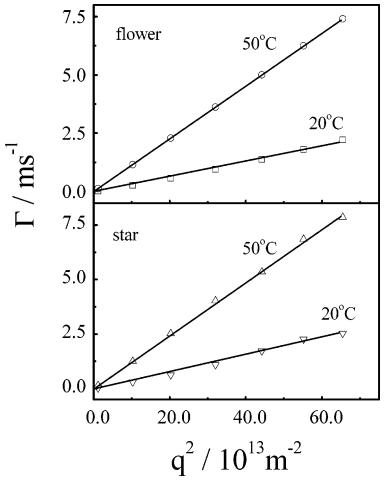

Figure 2. The typical scattering vector (q) dependence of the average line width ($\langle\Gamma\rangle$) of $PS_{30}-b$-$PNIPAM_{157}-b$-PS_{30} flower and star aggregates at 20 and 50 °C, where $C = 9.4 \times 10^{-6}$g/mL.

of gyration ($\langle R_g\rangle$), and the second virial coefficient (A_2) were determined to be 4.12×10^7 g/mol, 99 nm, and 2.4×10^{-7} mol cm^3/g^2. Similarly, for the $PS_{30}-b$-$PNIPAM_{39}-b$-PS_{30} aggregates before the hydrolysis, we have $M_{w,a} = 1.16 \times 10^8$ g/mol, $\langle R_g\rangle = 64$ nm, and $A_2 = 4.0 \times 10^{-8}$ mol cm^3/g^2. The small values of A_2 imply that water is a selective solvent for the aggregates. The aggregation number (N_{agg}) of the chains can be calculated using $N_{agg} = M_{w,a}/M_{w,b}$, where $M_{w,b}$ is the molecular weight of the triblock copolymer. For $PS_{30}-b$-$PNIPAM_{157}-b$-PS_{30} and $PS_{30}-b$-$PNIPAM_{39}-b$-PS_{30} aggregates, the aggregation numbers are 1720 and 10 906, respectively.

Note that the triblock copolymers form micelle-like aggregates instead of micelles. It is known that the maximum length of a chain is proportional to the total number of units and each unit has a length of 0.25 nm. For $PS_{30}-b$-$PNIPAM_{157}-b$-PS_{30} and $PS_{30}-b$-$PNIPAM_{39}-b$-PS_{30}, their maximum lengths are ~54 and ~24 nm, respectively. Assuming a triblock copolymer chain fold in two, the flower micelles formed by the two triblock copolymers should have a radius less than 27 and 12 nm, respectively. As discussed below, the measured radii of the aggregates are larger than these values, suggesting that the aggregates are not regular micelles where all PNIPAM blocks are strictly arranged in the corona. The morphology of block copolymer aggregates depends on polymer properties such as the structure, molecular weight, the relative block length, the chemical nature of the repeat unit, and the preparation conditions.[24,25] In the present study, when the copolymer chains are introduced to water, the hydrophobic PS blocks either in the same chain or in different chains would associate. Because the hydrophilic PNIPAM block is in the middle, while the chains undergo interchain aggregation, the individual chains also have chance to form PNIPAM rings interlocked each other by the associating PS blocks. Consequently, the interlocking PNIPAM rings pack not only in the corona but in the core with PS domains (Scheme 1). This explains why the triblock copolymers form a micelle-like aggregate larger than a regular micelle.

Figure 2 shows the typical scattering vector (q) dependence of the average line width ($\langle\Gamma\rangle$) for $PS_{30}-b$-$PNIPAM_{157}-b$-PS_{30} aggregates at different temperatures. It is known that amphiphilic BAB triblock copolymer with soluble middle A block and insoluble B blocks form single or multiflower micelles.[26,27] According to eq 4, for purely diffusive relaxation, $\langle\Gamma\rangle$ is linearly dependent on the square of the scattering vector (q), passing through the origin. Szczubialka et al.[28] show that $\langle\Gamma\rangle$ has a q^3-

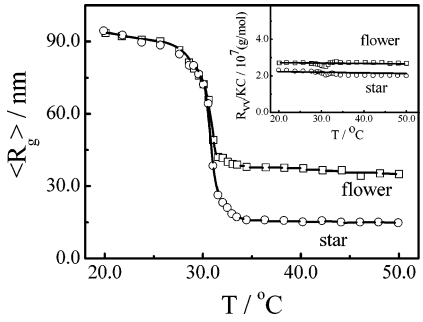

Figure 3. Temperature dependence average radius of gyration $\langle R_g\rangle$ of $PS_{30}-b$-$PNIPAM_{157}-b$-PS_{30} flower and star aggregates, where $C = 9.4 \times 10^{-6}$g/mL.

dependence if BAB triblock copolymers form a multiflower or bridged micelle. The linear relation of $\langle\Gamma\rangle$ versus q^2 shown in Figure 2 indicates that the aggregates at any a temperature in the range 20−50 °C, either before or after the hydrolysis, are isotropic diffusive. In the same way, we can know the $PS_{30}-b$-$PNIPAM_{39}-b$-PS_{30} aggregates are also isotropic diffusive. Moreover, as we discussed below, the hydrolysis only leads a slight change in the average radius gyration $\langle R_g\rangle$ and $R_{vv}(q)$, indicating that the aggregates are not bridged micelles. Otherwise, one aggregate would be cut into several smaller aggregates, leading to a great decrease in $\langle R_g\rangle$ and $R_{vv}(q)$. Thus, the aggregates formed by either of the triblock copolymers are spherical micelle-like. Namely, the aggregates are expected to be single-flower like before the hydrolysis and star-like after the hydrolysis at a temperature below the LCST of PNIPAM.

Figure 3 shows the temperature dependence of $\langle R_g\rangle$ of $PS_{30}-b$-$PNIPAM_{157}-b$-PS_{30} flower and star aggregates. In the range 20 °C to 30 °C, $\langle R_g\rangle$ almost does not change after the rings are cut into linear coils, indicating that the integrity of an aggregate has not been destroyed by the hydrolysis. In other words, the cutting mainly occurs in the PNIPAM rings in the corona. As temperature increases, $\langle R_g\rangle$ gradually decreases, indicating the aggregates with either rings or coils slowly shrink. In the range 30−32 °C, the sharp decrease in $\langle R_g\rangle$ clearly reveals the collapse of the aggregates. As temperature increases from 20 to 32 °C, $\langle R_g\rangle$ drops ~60 and 80 nm for the flower and star aggregates, respectively. Because the decrease in $\langle R_g\rangle$ is larger than the half of the maximal length of PNIPAM block (~20 nm), it cannot be attributed to the collapse of PNIPAM blocks in corona only. The collapse of PNIPAM blocks in the core also contributes to the decrease of $\langle R_g\rangle$. In the range 32−50 °C, as temperature increases, $\langle R_g\rangle$ slightly decreases to be a constant, indicating the full collapse of the aggregates. Obviously, the flower aggregates exhibit $\langle R_g\rangle$ larger than the star aggregates at the collapsed state. The difference is due to the different topological structures of the rings and coils in the corona. Since $\langle R_g\rangle$ is related to the chain density distribution in space, the larger $\langle R_g\rangle$ indicates that the rings are much less collapsed than the coils.

The inset shows that $R_{vv}(q)/KC$ only slightly drops after the cutting. Since $R_{vv}(q)$ is proportional to the weight-average molar mass of the aggregates, it is sensitive to the change of the aggregates. The slight change of $R_{vv}(q)/KC$ further indicates that most cut PNIPAM blocks are in the corona. Otherwise, the aggregate would be spilt, leading to a larger change in $R_{vv}(q)$. The inset also shows that $R_{vv}(q)/KC$ of the aggregates with either rings or coils do not have temperature dependence, indicating that the aggregates do not associate in the range we investigated. Namely, the aggregates show an individual behavior. As we know, PNIPAM chains readily aggregate at ~32 °C, so the tethered PNIPAM chains are more stable than the free PNIPAM

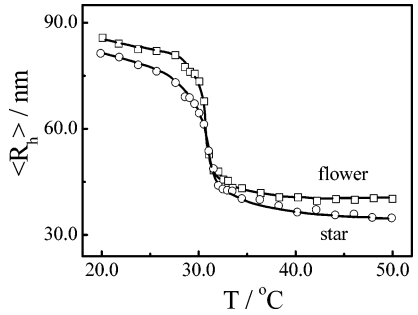

Figure 4. Temperature dependence of average hydrodynamic radius $\langle R_h \rangle$ of $PS_{30}-b$-$PNIPAM_{157}-b$-PS_{30} flower and star aggregates, where $C = 9.4 \times 10^{-6}$g/mL.

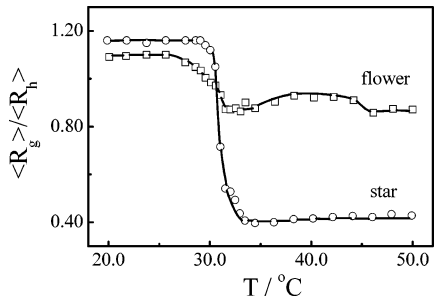

Figure 5. Temperature dependence of the ratio of the average hydrodynamic radius to the average radius of gyration ($\langle R_g \rangle / \langle R_h \rangle$) of $PS_{30}-b$-$PNIPAM_{157}-b$-PS_{30} flower and star aggregates, where $C = 9.4 \times 10^{-6}$g/mL.

chains. This phenomenon was first observed by Tenhu et al.[29] The reason is that the tethered chains have much smaller contact area than the free chains so that they have less chances to stick together.

Figure 4 shows the temperature dependence of $\langle R_h \rangle$ of $PS_{30}-b$-$PNIPAM_{157}-b$-PS_{30} flower or star aggregates. In the range 20 °C to 30 °C, both aggregates gradually shrink, but the former exhibit $\langle R_h \rangle$ slightly larger than that of the latter, suggesting that the rings in the corona are more stretched than the linear coils in the swollen state. This might be because more water is coupled and trapped in a close chain due to the topological effect. The sharp decrease in $\langle R_h \rangle$ in the range 30−32 °C further reveals the collapse of PNIPAM chains. In the range 32−50 °C, $\langle R_h \rangle$ slightly decreases to be a constant, implying that the aggregates are fully collapsed. The most important event is that the $\langle R_h \rangle$ of the flower aggregates is close to that of star aggregates in the collapsed state, indicating that the difference of dehydration between the rings and the coils is small.

Figure 5 shows the temperature dependence of $\langle R_g \rangle / \langle R_h \rangle$ of the $PS_{30}-b$-$PNIPAM_{157}-b$-PS_{30} aggregates. The conformation of a polymer chain or a structure of a particle can be described by their $\langle R_g \rangle / \langle R_h \rangle$. For random coil, hyperbranched cluster or micelle, and uniform sphere, $\langle R_g \rangle / \langle R_h \rangle$ is 1.5∼1.8, 1.0∼1.2, and ∼0.774, respectively.[30] In the present case, the star and flower aggregates have $\langle R_g \rangle / \langle R_h \rangle$ ∼1.15 and ∼1.10 at a temperature below ∼28 °C, respectively, indicating that both aggregates have a core−shell structure. Meanwhile, the slight change of $\langle R_g \rangle / \langle R_h \rangle$ before and after the hydrolysis indicates that the cutting mainly occurs in PNIPAM rings in the corona. This is because the cutting of PNIPAM rings in the core would change the structure of the aggregate, resulting in a larger change in $\langle R_g \rangle / \langle R_h \rangle$. Note that the flower aggregates have a smaller $\langle R_g \rangle / \langle R_h \rangle$ because they have a larger $\langle R_h \rangle$ due to the topological effect.

For the star aggregates, $\langle R_g \rangle / \langle R_h \rangle$ sharply decreases from 1.15 to 0.40 in the range 28−32 °C and leaves off at temperatures

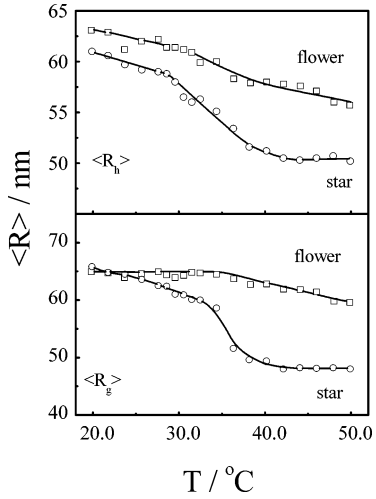

Figure 6. Temperature dependence of average radius of gyration $\langle R_g \rangle$ and average hydrodynamic radius $\langle R_h \rangle$ of $PS_{30}-b$-$PNIPAM_{39}-b$-PS_{30} flower and star aggregates, where $C = 9.4 \times 10^{-6}$g/mL.

above 32 °C, clearly indicating the aggregates collapse as temperature increases. The small $\langle R_g \rangle / \langle R_h \rangle$ value (∼0.40) indicates that the aggregates have a dense core. For the flower aggregates, $\langle R_g \rangle / \langle R_h \rangle$ exhibits a transition broader than that of the star aggregates. This is also attributed to the topological restriction. At a temperature above 32 °C, we originally expected that $\langle R_g \rangle / \langle R_h \rangle$ tends to be a constant, like what happened in the star aggregates. However, unexpected rise in $\langle R_g \rangle / \langle R_h \rangle$ can be observed in the range 33−46 °C. After a careful check of Figure 3 and Figure 4, we know that $\langle R_g \rangle$ and $\langle R_h \rangle$ gradually decrease in the range 33−46 °C, but $\langle R_h \rangle$ drops more than $\langle R_g \rangle$. As we discussed above, in the collapsed state, the rings are much less collapsed than the coils; namely, the former is in a so-called crumpled state, but they are dehydrated to almost the same level. The small rise in $\langle R_g \rangle / \langle R_h \rangle$ of flower aggregates is due to the less collapsed rings.

Figure 6 shows the temperature dependence of $\langle R_h \rangle$ and $\langle R_g \rangle$ of $PS_{30}-b$-$PNIPAM_{39}-b$-PS_{30} flower and star aggregates, respectively. $PS_{30}-b$-$PNIPAM_{39}-b$-PS_{30} triblock copolymer has two PS blocks the same as those in $PS_{30}-b$-$PNIPAM_{157}-b$-PS_{30}, but the former has a much shorter PNIPAM block. As temperature increases, $\langle R_h \rangle$ and $\langle R_g \rangle$ of $PS_{30}-b$-$PNIPAM_{39}-b$-PS_{30} aggregates decrease. As discussed above, because the decrease in $\langle R_g \rangle$ is larger than the half of the maximal length of PNIPAM block (∼5 nm), the decrease in the size is attributed to the collapse of PNIPAM blocks in both corona and core. In comparison with $PS_{30}-b$-$PNIPAM_{157}-b$-PS_{30} aggregates, $PS_{30}-b$-$PNIPAM_{39}-b$-PS_{30} aggregates exhibit more continuous collapse transition. This is because PNIPAM blocks are short, and their segments are more restricted on the PS surface.

Figure 7 shows the temperature dependence of $\langle R_g \rangle / \langle R_h \rangle$ of $PS_{30}-b$-$PNIPAM_{39}-b$-PS_{30} aggregates. For the star aggregates, $\langle R_g \rangle / \langle R_h \rangle \approx 1.07$ at temperature below 34 °C, indicating the core−shell structure of the aggregates. $\langle R_g \rangle / \langle R_h \rangle$ decreases from 1.06 to 0.96 in the range 34.5−36.5 °C, and tends to be a constant at temperatures above 37 °C, indicating the collapse of the aggregates. For flower aggregates, $\langle R_g \rangle / \langle R_h \rangle$ gradually increases from ∼1.03 to 1.09 at temperatures below ∼37 °C. This is due to the fact that $\langle R_h \rangle$ decreases more quickly than $\langle R_g \rangle$ (Figure 6); namely, the dehydration is some quicker than the collapse. At a temperature above ∼37 °C, $\langle R_g \rangle / \langle R_h \rangle$ slightly changes because the dehydration and collapse occur almost at the same pace.

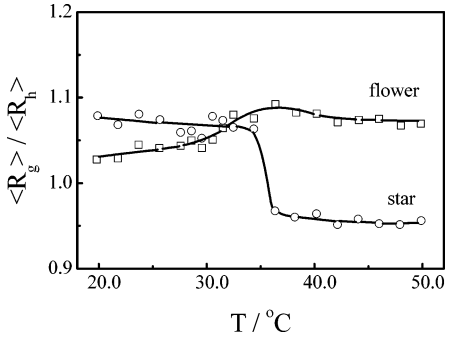

Figure 7. Temperature dependence of the ratio of the average hydrodynamic radius to the average radius of gyration ($\langle R_g \rangle / \langle R_h \rangle$) of $PS_{30}-b$-$PNIPAM_{39}-b$-PS_{30} flower and star aggregates, where $C = 9.4 \times 10^{-6}$g/mL.

Conclusion

The laser light scattering study on the temperature induced collapse of aggregates formed by polystyrene−*b*-poly(*N*-isopropylacrylamide)−*b*-polystyrene (PS−*b*-PNIPAM−*b*-PS) triblock copolymers leads to the following conclusions. The triblock copolymer chains form flower-like aggregates in water with PNIPAM interlocking rings and associating PS blocks as the core and PNIPAM rings as the corona. The aggregates can be readily transformed into star aggregates with open coils as the corona by hydrolyzing the trithiocarbonate groups. The flower aggregates are much less collapsed than the star aggregates due to the topological effect of PNIPAM blocks in the corona. The star aggregates with long coils exhibit a sharper collapse transition than the aggregates with shorter coils.

Acknowledgment. The financial support of National Natural Science Foundation (NNSF) of China (20474060) and The Chinese Academy of Sciences (KJCX2-SW-H14) is gratefully acknowledged.

References and Notes

(1) Alexander, S. *J. Phys. (Paris)* **1977**, *38*, 983.
(2) de Gennes, P. G. *Macromolecules* **1980**, *13*, 1069.
(3) Halperin, A.; Tirrell, M.; Lodge, T. P. *Adv. Polym. Sci.* **1991**, *100*, 31.
(4) Milner, S. T. *Science* **1991**, *251*, 905.
(5) Birshtein, T.; Amoskov, V. *Polym. Sci., Ser. C* **2000**, *42*, 172.
(6) Zhulina, E. B.; Borisov, O. V.; Pryamitsyn, V. A.; Birshtein, T. M. *Macromolecules* **1991**, *24*, 140.
(7) Grest, G. S.; Murat, M. In *Monte Carlo and Molecular Dynamics Simulations in Polymer Science*; Binder K., Ed.; Clarendon: Oxford, 1994.
(8) Yakubov, G. E.; Loppinet, B.; Zhang, H.; Rühe, J.; Sigel, R.; Fytas, G. *Phys. Rev. Lett.* **2004**, *92*, 115501. Domack, A.; Prucker, S.; Rühe, J.; Johannsmann, D. *Phys. Rev. E* **1997**, *56*, 680.
(9) Karim, A.; Satija, S. K.; Douglas, J. F.; Ankner, J. F.; Fetters, L. J. *Phys. Rev. Lett.* **1994**, *73*, 3407.
(10) Balamurugan, S.; Mendez, S.; Balamurugan, S. S.; O' Brien, M. J. II; Lopez, G. P. *Langmuir* **2003**, *19*, 2545. Yim, H.; Kent, M. S. Mendez, S.; Balamurugan, S. S.; Balamurugan, S.; Lopez, G. P.; Satija, S. *Macromolecules* **2004**, *37*, 1994.
(11) Zhu, P. W.; Napper, D. H. *Langmuir* **1996**, *12*, 5992.
(12) Takei, Y. G.; Aoki, T.; Sanui, K.; Ogata, N.; Sakurai, Y.; Okano, T. *Macromolecules* **1994**, *27*, 6163.
(13) Zhang, J.; Pelton, R.; Deng, Y. *Langmuir* **1995**, *11*, 2301.
(14) Zhang, W. A.; Zhou, X. C.; Li, H.; Fang, Y.; Zhang, G. Z. *Macromolecules* **2005**, *38*, 909.
(15) Alberts, B.; Bray, D.; Lewis, J.; Raff, M.; Roberts, K.; Watson, J. D. *Molecular Biology of the Cell*; Garland Publishing: New York, 1994.
(16) Mayadunne, R. T. A.; Rizzardo, E.; Chiefari, J.; Krstina, J.; Moad, G.; Postma, A.; Thang, S. H. *Macromolecules* **2000**, *33*, 243.
(17) Lai, J. T.; Filla, D.; Shea, R. *Macromolecules* **2002**, *35*, 6754.
(18) Liu, J.; Hong, C. Y.; Pan, C. Y. *Polymer* **2004**, *45*, 4413.
(19) Zhu, M. Q.; Wang, L. Q.; Exarhos, G. J.; Li, A. D. Q. *J. Am. Chem. Soc.* **2004**, *126*, 2656.
(20) Zimm, B. H. *J. Chem. Phys.* **1948**, *16*, 1099.
(21) Chu, B. *Laser Light Scattering*, 2nd ed.: Academic Press: New York, 1991.
(22) Berne, B.; Pecora, R. *Dynamic Light Scattering*; Plenum Press: New York, 1976.
(23) Xia, J.; Dubin, P. In *Macromolecular Complexes in Chemistry and Biology*; Dubin, P., Bock, J., Davies, R. M., Schultz, D. N., Thies, C., Eds.; Spring-Verlag: New York, 1994; p 247.
(24) Terreau, O.; Luo, L. B.; Eisenberg, A. *Langmuir* **2003**, *19*, 5601.
(25) Choucair, A.; Eisenberg, A. *Eur. Phys. J. E* **2003**, *10*, 37.
(26) Halperin, A. *Macromolecules* **1991**, *24*, 1418. Borisov, O. V.; Halperin, A. *Macromolecules* **1996**, *29*, 2612.
(27) Lee, N. K.; Abrams, C. F. *J. Chem. Phys.* **2004**, *121*, 7484.
(28) Szczubialka, K.; Ishikawa, K.; Morishima, Y. *Langmuir* **2000**, *16*, 2083.
(29) Shan, J.; Chen, J.; Nuopponen, M.; Tenhu, H. *Langmuir* **2004**, *20*, 4671. Nuopponen, M.; Ojala, J.; Tenhu, H. *Polymer* **2004**, *45*, 3643.
(30) Burchard, W. In *Light Scattering Principles and Development*; Brown, W., Ed.; Clarendon Press: Oxford, 1996; p 439.